respectively. Qualitatively this is reasonable. The transition state for k_r^O is conformer **3** of Scheme I, corresponding to a stable minimum of the threefold barrier for rotation about the C–N bond. The transition state for k_r^R is a conformer corresponding to the top of that barrier. The energy difference between these two transition states is the 3-fold component of the rotational barrier. By analogy to methyl rotors on a double bond, that energy difference may be expected to be ca. 1 kcal/mol.[14,29] However, detailed analysis[42] of Scheme III shows that our observed rate constants for cyanoacetamide, malonamide, ethyl oxamate, chloroacetamide, and dichloroacetamide require that this energy difference be only 0.6, 0.2, −0.4, 0.2, and −0.13 kcal/mol, respectively. Not only are some of these energy differences negative, corresponding to the necessity that **3** be a conformation of maximum energy, but also they are too small, appreciably less than 1 kcal/mol. To account for the observed rate ratios, it is necessary that the 3-fold component of the rotational barrier must have nearly vanished, which is unreasonable.

Furthermore, to account for the near absence of intramolecular exchange in these amides, it is necessary to assume that k_d/k_r has been increased for amides with electron-withdrawing substituents. Since k_r^O and k_r^R are required by the data to be nearly equal, they must both be quite high. Therefore the increase in k_d/k_r cannot be due to a decrease in k_r. It is necessary to conclude[24] that k_d has increased for amides with electron-withdrawing substituents, even though this is a diffusion-controlled deprotonation and should be independent of amide.

Thus invoking the N-protonation mechanism for these amides leads to three unlikely requirements—a substantial 6-fold barrier to C–N rotation, disappearance and occasional reversal of the 3-fold component of that barrier, and substituent effects on the rate constant for a diffusion-controlled deprotonation. We therefore conclude that these results for amides with electron-withdrawing substituents are consistent only with the imidic acid mechanism. Thus we have at last obtained evidence for the mechanism that we had originally though to be the more attractive one, even though we have been surprised to find that it is not the dominant mechanism for primary amides.

Acknowledgment. This research was supported by National Science Foundation Grants CHE76-02408 and CHE78-12246. We thank Dr. John Wright for assistance with the NMR spectrometers, which were supported by National Institutes of Health Grant RR-708. We are indebted to Mr. Paul A. Kobrin for some of the line-broadening measurements.

(42) Perrin, C. L., unpublished calculations.

Experimental Chemical Shift Correlation Maps from Heteronuclear Two-Dimensional NMR Spectroscopy. 1. Carbon-13 and Proton Chemical Shifts of Raffinose and Its Subunits

Gareth A. Morris† and Laurence D. Hall*

Contribution from the Department of Chemistry, University of British Columbia, Vancouver, British Columbia, Canada V6T 1W5. *Received December 27, 1979*

Abstract: With the use of double Fourier transform ("2D") NMR methods it is possible to make a simultaneous measurement of proton and carbon-13 chemical shifts for each directly bonded carbon–proton pair in a molecule. Correlation of proton and carbon-13 shifts greatly increases the information capacity of NMR experiments, allowing otherwise inaccessible proton shifts to be determined and facilitating assignment. Experimental results are presented for raffinose, melibiose, sucrose, galactose, glucose, and fructose; the carbon-13 spectra of raffinose and melibiose are reassigned, and proton shifts are reported for all three significant solution forms of aqueous fructose.

Two of the fundamental problems in NMR are the measurement of NMR parameters from complex crowded spectra and the assignment of these resonances to specific nuclear sites in a molecule. Advances in instrumentation have improved sensitivity more rapidly than resolving power, with the result that the complexity of the system which may be studied by abundant spin NMR is now limited largely by the problem of resolving and identifying single resonances. Since the amount of information to be gleaned from the measurement of the chemical shift of a resonance is limited, techniques such as double-resonance and relaxation-time measurement have increasingly been adopted. By *correlating* two independent parameters such as the chemical shift of a resonance and the chemical shift of a second nucleus scalar coupled to the first (as in double resonance), the specificity with which a resonance may be characterized and hence the ease of its assignment can be greatly enhanced. Double-resonance methods such as homonuclear INDOR also attack the problem of spectral overcrowding by allowing "hidden" resonances to be detected.

In recent years a number of new techniques have been developed, based on the double Fourier transformation of NMR signals, which attack the problems of resolving individual signals and correlating NMR parameters in a very direct way. Such experiment, commonly referred to by the generic title of two-dimensional or "2D" NMR spectroscopy,[1,2] produce spectra which display signal strength as a function of two independent frequencies. The choice of which NMR parameters are responsible for spreading resonances in each frequency domain is under the control of the experimenter, through his choice of pulse sequence for the acquisition of the time domain data for double Fourier transformation.

The purpose of this paper is to illustrate the application of one 2D NMR experiment, for the correlation of proton and carbon-13

† Physical Chemistry Laboratory, Oxford University, South Parks Road, Oxford OX1 3QZ, England

(1) (1) Aue, W. P.; Bartholdi, E.; Ernst, R. R. *J. Chem. Phys.* **1976**, *64*, 2229–46.
(2) Freeman, R.; Morris, G. A. *Bull. Magn. Reson.* **1979**, *1*, 5–26.

0002-7863/81/1503-4703$01.25/0

chemical shifts, to a series of carbohydrates. Although they have been extensively studied, the NMR spectra of raffinose and its constituent mono- and disaccharides have still not all been fully analyzed, and offer some nice illustrations of the problems often encountered in proton and carbon-13 NMR. The carbon-13 spectra of the monosaccharides galactose (I), glucose (II), and

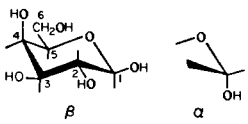

I

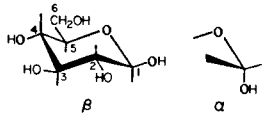

II

fructose (III) now have well-established assignments,[3] as does that

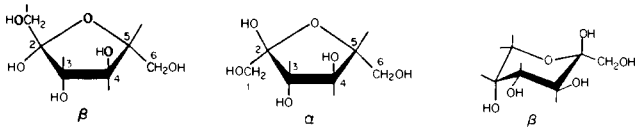

III

of sucrose (V), the disaccharide α-D-glucopyranosyl-(1→2)-β-D-fructofuranose. For meliboise (IV) (α-D-galactopyranosyl-(1→6)-α-D-glucopyranose) and raffinose (VI) (α-D-galacto-

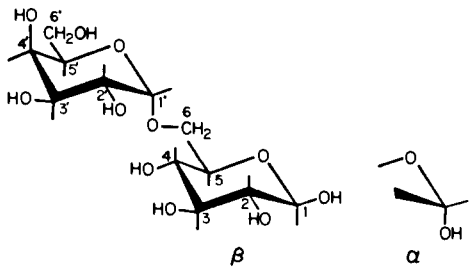

IV

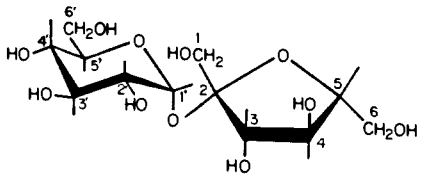

V

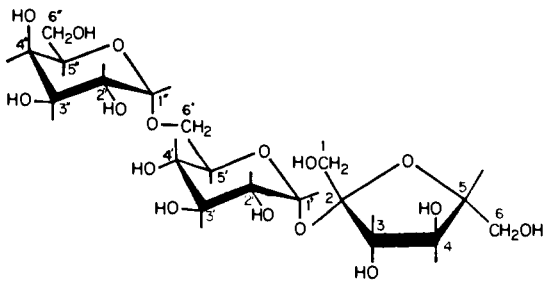

VI

pyranosyl-(1→6)-α-D-glucopyranosyl-(1→2-β-D-fructofuranose), however, only very early attempts at assignment are available.[4,5] These tentative assignments of necessity relied heavily on comparison between the carbon-13 chemical shifts of mono- and oligosaccharides, and hence tended to fall foul of the fairly large carbon-13 shift changes that can attend the formation of glycosidic linkages.

The proton NMR spectra of the three monosaccharides are surprisingly difficult to interpret for comparatively small molecules. The two main problems are the presence of more than one form of each sugar at equilibrium in aqueous solution, and the relatively small range of chemical shifts found for the nonanomeric protons, leading to crowded and strongly coupled spectra. In addition, even when all the parameters of the spin system can be extracted from the spectrum there remains an assignment problem, since many of the ring proton–proton coupling constants are very similar. One approach that has been successfully applied to glucose[6] is to use iterative computer analysis of the conventional proton spectrum; in spectra any more crowded than glucose, however, this method suffers as a result of the difficulty of resolving single resonances. All of the systems studied have also been investigated by continuous wave 300 MHz INDOR,[7-11] shifts being reported for all weakly coupled protons in I, II, IV, V, and VI and for the major resonances of fructose[8] (III).

The measurement of correlated proton chemical shifts from a series of off-resonance decoupled carbon-13 spectra is now routine practice.[12-16] Unfortunately strong coupling effects[16,17] and radio frequency field inhomogeneity[18] often lead to misleading multiplet patterns, necessitating long experiments in order to obtain the good signal-to-noise ratio needed for each carbon-13 spectrum. Under favorable conditions an accuracy of about ±0.1 ppm is attainable for proton shifts measured by this method, although interpretation is often difficult in crowded spectra, but the time needed to record all the necessary off-resonance decoupled spectra can easily amount to several hundred times that needed for a single wideband decoupled spectrum.

Two-dimensional spectroscopy can offer a faster and more accurate alternative. The heteronuclear chemical shift correlation experiment, described in more detail in the next section, provides a two-dimensional spectrum in which one frequency axis displays signals as a function of carbon-13 chemical shift, and the other dimension disperses signals according to their proton chemical shift. One signal appears for each directly bonded carbon–proton pair in a molecule, the coordinates of the signal in the 2D spectrum being just the carbon-13 and proton chemical shift frequencies.

Chemical Shift Correlation by Heteronuclear Two-Dimensional NMR

In double Fourier transform, or 2D, NMR a series of free induction decays $S(t_2)$ is excited by a pulse sequence containing an interval t_1, which is varied in equal steps until a matrix $S(t_1,t_2)$ has been built up which describes the total nuclear signal as a function both of the time t_2 after excitation and of the delay t_1 during the exciting pulse sequence. Just as a single Fourier transformation sorts out the frequency components of a free induction decay, so a double transformation of the matrix $S(t_1,t_2)$ produces a two-dimensional spectrum $S(f_1,f_2)$ in which signals are dispersed in f_2 according to their oscillation frequency during acquisition of the free induction decays and dispersed in f_1 according to their apparent frequency of oscillation during t_1. The interested reader is referred to ref 2 for a survey of the many pulse

(3) (a) Pfeffer, P. E.; Valentine, K. M.; Parrish, F. W. *J. Am. Chem. Soc.* **1979**, *101*, 1265–74. (b) Angyal, S. J.; Bethell, G. S. *Aust. J. Chem.* **1976**, *29*, 1249–65.

(4) Breitmaier, E.; Voelter, W. "^{13}C Spectroscopy: Methods and Applications"; Verlag Chemie: New York, 1978; p 260.

(5) Allerhand, A.; Doddrell, D. *J. Am. Chem. Soc.* **1971**, *93*, 2777–9.

(6) Perkins, S. J.; Johnson, L. N.; Phillips, D. C.; Dwek, R. A. *Carbohydr. Res.* **1977**, *59*, 19–34.

(7) DeBruyn, A.; Anteunis, M.; Verhegge, G. *Acta Cienc. Indica* **1975**, *1*, 83–5.

(8) DeBruyn, A.; Anteunis, M.; Verhegge, G. *Carbohydr. Res.* **1975**, *41*, 295–7.

(9) DeBruyn, A.; Van Beeumen, J.; Anteunis, M.; Verhegge, G. *Bull. Soc. Chim. Belg.* **1975**, *84*, 799–811.

(10) DeBruyn, A.; Anteunis, M.; Van Beeumen, J.; Verhegge, G. *Bull. Soc. Chim. Belg.* **1975**, *84*, 407–16.

(11) Anteunis, M.; DeBruyn, A.; Verhegge, G. *Carbohydr. Res.* **1975**, *44*, 101–5.

(12) Freeman, R.; Hill, H. D. W. *J. Chem. Phys.* **1971**, *54*, 3367–77.

(13) Tanabe, M.; Hamasaki, T.; Thomas, D.; Johnson, L. F. *J. Am. Chem. Soc.* **1971**, *93*, 273–4.

(14) Birdsall, B.; Birdsall, N. J. M.; Feeney, J. *J. Chem. Soc., Chem. Commun.* **1972**, 316–7.

(15) MacDonald, J. C.; Mazurek, M. *J. Magn. Reson.* **1977**, *28*, 181–90.

(16) Wehrli, F. W.; Wirthlin, T. "Interpretation of Carbon-13 NMR Spectra"; Heyden: London, 1976.

(17) Grutzner, J. B. *J. Chem. Soc., Chem. Commun.* **1974**, 64.

(18) Freeman, R.; Grutzner, J. B.; Morris, G. A.; Turner, D. L. *J. Am. Chem. Soc.* **1978**, *100*, 5637–40.

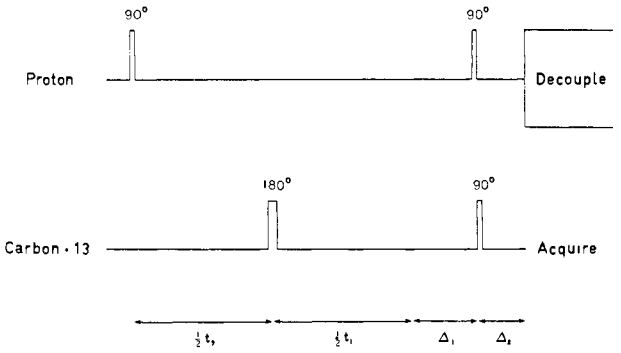

Figure 1. Pulse sequence used for obtaining heteronuclear chemical shift correlation 2D spectra. For the experiments described Δ_1 was 3 ms and Δ_2 was 2.2 ms.

sequences currently in use, and for a discussion of the technical details of double Fourier transform NMR experiments.

The aim of a pulse sequence for carbon–proton chemical shift correlation is then to generate carbon-13 free induction decays in which each decoupled carbon-13 signal has been made to oscillate for a period t_1 at the chemical shift frequency of any proton to which that carbon nucleus is directly bonded. This effect can be achieved by the pulse sequence of Figure 1, in which the proton decoupler is used to provide first coherent 90° proton pulses and then wideband proton decoupling.

The operation of the pulse sequence of Figure 1 is most easily followed for a simple carbon–proton AX spin system, which has two carbon-13 resonances (the proton-coupled carbon-13 spectrum) and two proton resonances (the carbon-13 satellites in the proton spectrum). The energy level diagram for this system is shown in Figure 2, together with the carbon-13 and proton spectra and the spin state populations at Boltzmann equilibrium. The initial 90° proton pulse of Figure 1 will create two transverse proton magnetizations, one due to coherence between spin states 1 and 3, and one due to that between 2 and 4.

Free precession now takes place for a period of $0.5t_1$, at which time the carbon-13 180° pulse flips all the carbon-13 spins α for β, so that the magnetizations interchange resonant frequencies. Further free precession now takes place for a period $0.5t_1 + \Delta_1$, so that immediately before the second proton 90° pulse the two magnetizations may be written:

$$M_{xy}^{13}(t_1 + \Delta_1) = iM_H^0 \exp\{-2\pi i\delta_H(t_1 + \Delta_1)\} \exp(+\pi iJ_{CH}\Delta_1)$$

$$M_{xy}^{24}(t_1 + \Delta_1) = iM_H^0 \exp\{-2\pi i\delta_H(t_1 + \Delta_1)\} \exp(-\pi iJ_{CH}\Delta_1) \quad (1)$$

where M_H^0 is the initial proton polarization. The second proton 90° pulse will now rotate these magnetizations by 90° about the proton transmitter field in the proton rotating frame, converting their imaginary parts into longitudinal magnetization.

Since longitudinal magnetization is directly proportional to the spin state population difference across a transition, the net result of the pulse sequence so far has been to modulate the populations P_1–P_4 of the four states as a function of t_1. The differential "pumping" of the spin state populations by the proton pulse sequence thus gives a t_1 dependence to the population differences across the carbon-13 transitions. By once again using the equivalence between population difference and longitudinal magnetization, the carbon-13 90° pulse will generate two transverse magnetizations, one due to coherence between levels 1 and 2 and the other between 3 and 4:

$$M_{xy}^{12}(t_1 + \Delta_1) = -iM_C^0 - iM_H^0 \cos\{2\pi\delta_H(t_1 + \Delta_1)\} \sin(\pi J_{CH}\Delta_1)$$

$$M_{xy}^{34}(t_1 + \Delta_1) = -iM_C^0 + iM_H^0 \cos\{2\pi\delta_H(t_1 + \Delta_1)\} \sin(\pi H_{CH}\Delta_1) \quad (2)$$

where M_C^0 is the equilibrium Boltzmann carbon-13 polarization. The reason for the delay Δ_1 is now clear; without it the pairs of levels 1 and 2 and 3 and 4 would have their populations modulated in sympathy, so that there would be no effect on M^{12} and M^{34}. When Δ_1 is set to $1/(2J_{CH})$, as first pointed out by Ernst,[19] the depth of modulation of the carbon-13 signals is at a maximum. Because of the limited range of one-bond proton–carbon coupling constants encountered, a single compromise value of Δ_1 suffices to ensures adequate transfer of t_1 modulation to all protonated carbons.

Similarly, a second delay Δ_2 is added between the carbon-13 90° pulse and the onset of decoupling, in order to prevent the two antiphase components of eq 2 from cancelling. The resultant carbon-13 signal data acquisition is then:

$$M_{xy}^{C} = [-2M_C^0 \cos(\pi J_{CH}\Delta_2) + 2M_H^0 \sin(\pi J_{CH}\Delta_2) \times \cos\{2\pi\delta_H(t_1 + \Delta_1)\} \sin(\pi J_{CH}\Delta_1)] \exp\{-2\pi i\delta_C(t_2 + \Delta_2)\} \quad (3)$$

If the delays Δ_1 and Δ_2 are chosen equal to $1/(2J_{CH})$, eq 3 is greatly simplified, the t_1 modulation being at its maximum and the unmodulated signal due to the equilibrium carbon-13 polarization M_C^0 being lost:

$$M_{xy}^{C} = 2M_H^0 \cos\{2\pi\delta_H(t_1 + \Delta_1)\} \exp\{-2\pi i\delta_C(t_2 + \Delta_2)\} \quad (4)$$

which achieves the goal of producing decoupled carbon-13 free induction decay modulated as a function of t_1 by the proton chemical shift δ_H. Double Fourier transformation of a matrix of free induction decays obtained with different values of t_1 will result in a two-dimensional spectrum with peaks at $(+\delta_H,\delta_C)$ and $(-\delta_H,\delta_C)$, the shift correlation spectrum being symmetrical in frequency and intensity about the axis $F_1 = 0$, since the carbon-13 signal is amplitude modulated by the proton shift.

The vital step in the pulse sequence is the transfer of the t_1 modulation from protons to carbon-13 effected by the proton and carbon-13 90° pulse. The population arguments outlined above, introduced in ref 20, suffice to describe the behavior of the carbon-13 signals in heteronuclear chemical shift correlation. There is, however, a more general way of analyzing the modulation transfer, due to Ernst and co-workers,[21] in terms of a direct transfer of coherence from one pair of energy levels to another. The combined effect of the proton and carbon-13 90° pulses is to "punch through" the components of the proton magnetizations that lie along the y axis in the proton-rotating frame into the y axis of the carbon-rotating frame, the x axes in the two frames being defined by the proton and carbon-13 transmitter phases, respectively. At first sight this transfer of coherence may seem unfamiliar, but the phenomenon underlies many of the effects seen in the Fourier transform NMR, including echo modulation[22] and the dependence of the relative intensities within a spectrum on the flip angle of the observing pulse.[23] A particularly simple illustration of coherence transfer has recently been published,[24] making use of selective excitation[25] to generate a single carbon-13 coherence and then using a selective decoupler pulse to transfer this to a different carbon-13 transition.

Returning to the pulse sequence of Figure 1, the arguments used above may easily be extended to AX_2 and AX_3 systems, the only difference being that the optimum value for Δ_2 decreases slightly; again a compromise setting will ensure good polarization transfer for all protonated carbons. In the experiments to be described, the values of Δ_1 and Δ_2 used were 3 ms and 2.2 ms, respectively. The behavior of more complex spin systems is considerably more difficult to analyze, particularly where one or both of the carbon-13 satellites in the proton spectrum is strongly coupled. In weakly coupled systems homonuclear couplings among the protons will lead to fine structure in the f_1 domain of the 2D

(19) Maudsley, A. A.; Kumar, A.; Ernst, R. R. *J. Magn. Reson.* **1977**, *28*, 463–9.
(20) Bodenhausen, G.; Freeman, R. *J. Magn. Reson.* **1977**, *28*, 471–6.
(21) Maudsley, A. A.; Ernst, R. R. *Chem. Phys. Lett.* **1977**, *50*, 368–72.
(22) Hahn, E. L.; Maxwell, D. E. *Phys. Rev.* **1951**, *84*, 1246–1247.
(23) Schäublin, S.; Höhener, A.; Ernst, R. R. *J. Magn. Reson.* **1974**, *13*, 196–216.
(24) Henrichs, P. M.; Schwartz, L. J. *J. Magn. Reson.* **1977**, *28*, 477–80.
(25) Morris, G. A.; Freeman, R. *J. Magn. Reson.* **1978**, *29*, 433–62.

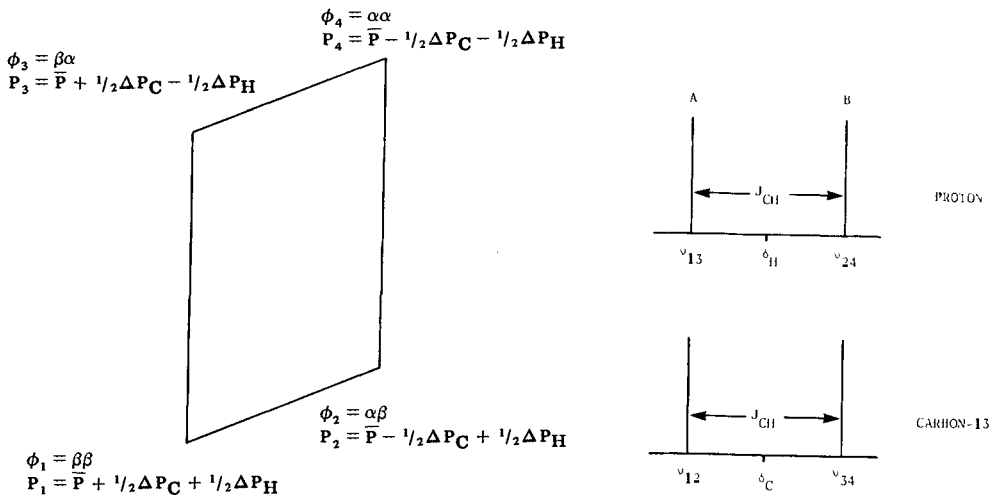

Figure 2. Energy levels, wave functions, equilibrium spin state populations, and stick spectra for a proton–carbon-13 AX spin system.

Table I. Carbon-13 and Proton Chemical Shifts for I to VI[a]

	carbon-13, ppm from external Me_4Si						proton, ppm from internal TSP					
	1	2	3	4	5	6	1	2	3	4	5	6
					D-Galactose (I)							
α-pyranose	93.10	69.17	69.99	70.13	71.28	62.01	5.26	3.78[a]	3.91	3.78	4.08	3.73
β-pyranose	97.28	72.69	73.62	69.56	95.96	61.80	4.58	3.48	3.65	3.93	3.70	3.76
					D-Glucose (II)							
α-pyranose	92.89	72.28	73.58	70.44	72.24	61.40	5.24	3.52[a]	3.71	3.40	3.82[a]	3.77, 3.44[a]
β-pyranose	96.71	74.94	76.74	70.40	76.56	61.57	4.64	3.25	3.46	3.40	3.47	3.86[a]
					D-Fructose							
α-furanose	63.77	105.24	82.81	76.90	82.15	61.94	3.66		4.11	3.99	4.04	3.86, 3.64[a]
β-furanose	63.56	102.31	76.28	75.32	81.51	63.20	3.57		4.11	4.10	3.82	3.79, 3.64[a]
β-pyranose	64.75	98.87	68.42	70.51	70.02	64.18	3.70, 3.54[a]		3.79	3.89	3.99	4.01, 3.69[a]
					Melibiose (IV)							
galactopyranosyl	99.02, 98.98[b]	69.28	70.30	70.03	71.75	61.93	5.00	3.83	3.93	4.02[a]	4.01	3.76
α-glucopyranose	93.00	72.25	73.76	70.41	70.91	66.76	5.26	3.56	3.72	3.48[a]	4.03	3.96, 3.75[a]
β-glucopyranose	96.88	74.87	76.70	70.26	75.16	66.67	4.69	3.27	3.51	3.52[a]	3.66	3.96, 3.75[a]
					Sucrose (V)							
glucopyranosyl	92.97	71.87	73.37	70.01	73.19	60.92	5.40	3.54	3.76	3.47	3.82	3.81
fructofuranose	62.13	104.48	77.19	74.78	82.12	63.17	3.67		4.21	4.04	3.89	3.81
					Raffinose (VI)							
galactopyranosyl	99.29	69.30	70.25	70.03	71.83	61.94	4.99	3.83	3.91[a]	4.00	3.96	3.75
glucopyranosyl	92.90	71.77	73.48	70.25	72.21	66.72	5.43	3.56	3.77	3.53[a]	4.04	4.01, 3.69[a]
fructofuranose	62.23	104.60	77.16	74.81	82.15	63.27	3.66		4.22	4.06	3.89	3.77[a]

[a] Estimated standard deviation 0.02 ppm. [b] α, β respectively. [c] Estimated standard deviation on shift values 0.01 ppm unless otherwise noted.

spectrum which mirrors the normal proton multiplet, while strong coupling in either carbon-13 satellite will distort the fine structure. Fortunately such effects do not interfere significantly with the operation of the basic experiment, the f_1 signal in the 2D spectrum remaining centered on the proton shift. Under normal operating conditions, such as those used in obtaining the results described below, proton–proton couplings are rarely resolved in f_1 and have little influence on the accuracy of the proton shifts measured. An analysis of homonuclear coupling effects in some related heteronuclear 2D experiments is given in ref 26. The theory and practice of heteronuclear 2D correlation experiments are discussed in ref 2, 19–21, and 26–29.

Experimental Section

The basic sequence of events in obtaining correlated proton and carbon-13 chemical shifts by 2D NMR is as follows. Time-averaged carbon-13 free induction decays of 1024 or 2048 points (depending on the f_2 digital resolution necessary in order to resolve all decoupled carbon-13 lines) were accumulated, using the pulse sequence of Figure 1, for 128 different values of t_1. This led to total data acquisition times for the 2D spectra of 30 to 150 min, compared with 2 to 15 min for obtaining proton decoupled carbon-13 spectra from the same samples. A spectral width of 1000 Hz was selected for f_1, sufficient to include the proton signals of all the systems studied, necessitating an increment of 500 μs between successive t_1 values. Each decay was then weighted exponentially and Fourier transformed, to yield a set of f_2 spectra for different t_1 values. The time constant for exponential weighting was chosen to be the shorter of the free induction decay acquisition times and the apparent T_2 of the signals, in order to ensure optimum sensitivity for the final 2D spectrum. The matrix $S(t_1,f_2)$ was transposed to yield a set of complex interferograms $S(t_1)$, one for each point in the digitized carbon-13 spectrum (i.e., one interferogram for each f_2 value). When a full 2D spectrum (such as Figure 4) was required, these interferograms were then Fourier transformed without further manipulation, and one half of the resultant 2D spectrum $S(f_2,f_1)$ was plotted.

In order to make the fullest use of the proton chemical shift data made available by these experiments, a slightly more complex course of action was used for obtaining numerical results. Interferograms were extracted from the matrix $S(f_2,t_1)$ at the carbon-13 chemical shift frequencies and zero filled three times prior to Fourier transformation, 896 zeroes being

(26) Bodenhausen, G.; Bolton, P. H., submitted for publication.
(27) Bodenhausen, G.; Freeman, R. *J. Am. Chem. Soc.* **1978**, *100*, 320–1.
(28) Freman, R.; Morris, G. A. *J. Chem. Soc., Chem. Commun.* **1978**, 684–6.
(29) Odenhausen, G.; Bolton, P. H. *J. Am. Chem. Soc.* **1979**, *101*, 1080–4.

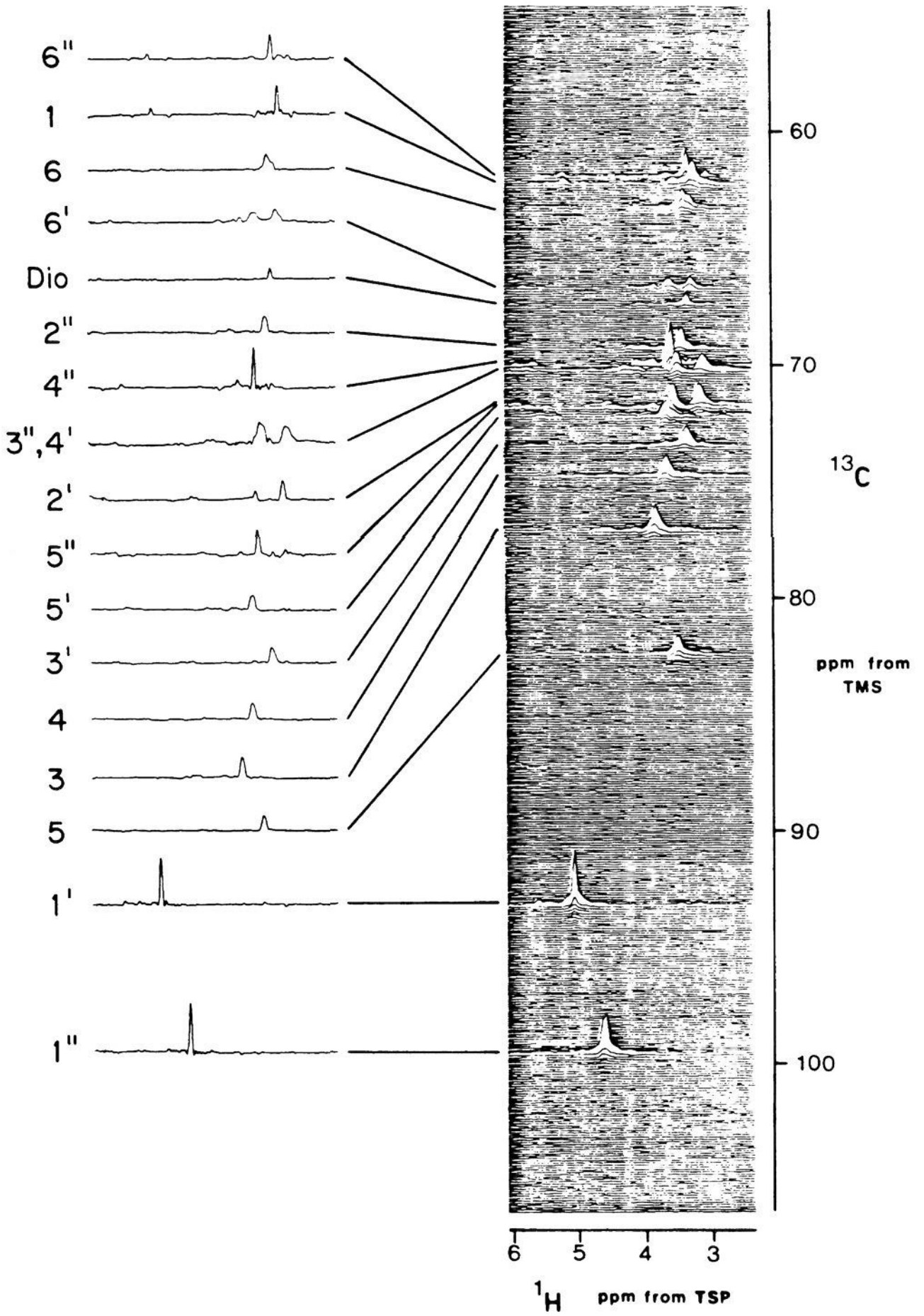

Figure 3. Stacked plot of a chemical shift correlation 2D spectrum of raffinose (VI) in D_2O, showing signal strength as a function of carbon-13 chemical shift (vertical or f_2 axis) and of proton chemical shift (horizontal or f_1 axis). Traces bearing signals have been recalculated, using zero-filling to improve digital resolution, and are displayed to the left of the full 2D spectrum.

appended to the 128 point real and imaginary components of the interferograms. For well-resolved signals this procedure improves the accuracy of line position measurement,[30] even though no true improvement in information content is obtained by zero filling more than once;[31] the extra points added by further zero filling serve to digitize better the (sin x/x) convoluted line shape in f_1. This leads to the characteristic "wiggles" seen on many of the f_1 traces to be presented in the next section.

The traces obtained are cross-sections through the f_1 domain of the 2D spectrum[32] and are symmetrical in frequency and intensity about the axis $f_1 = 0$; however, in an inhomogeneous static magnetic field signals which have the same sign of frequency in f_1 and f_2 will be broader than those with opposite signs, due to coherence transfer echoes.[33] Consequently the negative frequency halves of the f_1 traces were chosen for plotting and measurement, peak positions being determined with a standard parabolic interpolation routine. Traces were examined and plotted in phase-sensitive mode, except where the presence of overlapping resonances with strongly frequency-dependent phase shifts caused problems. Proton chemical shifts were measured from the traces by using *p*-dioxane (3.76 ppm from internal TSP) as reference, while carbon-13 shifts were measured from conventional decoupled spectra, again using dioxane (67.40 ppm from external Me_4Si) as a reference.

Experiments were performed on a home-built superconducting spectrometer operating at 270 and 67.9 MHz for carbon-13, based on a Nicolet/Bruker TT-23 console. Data acquisition and all the data processing operations described above were carried out by using the standard

(30) Comisarow, M. B.; Melka, J. D. *Anal. Chem.* **1979**, *51*, 2198–203.
(31) Bartholdi, E.; Ernst, R. R. *J. Magn. Reson.* **1973**, *11*, 9–19.
(32) Nagayama, K.; Bachmann, P.; Wüthrich, K.; Ernst, R. R. *J. Magn. Reson.* **1978**, *31*, 133–48.
(33) Baker, E. B. *J. Chem. Phys.* **1962**, *37*, 911–2.

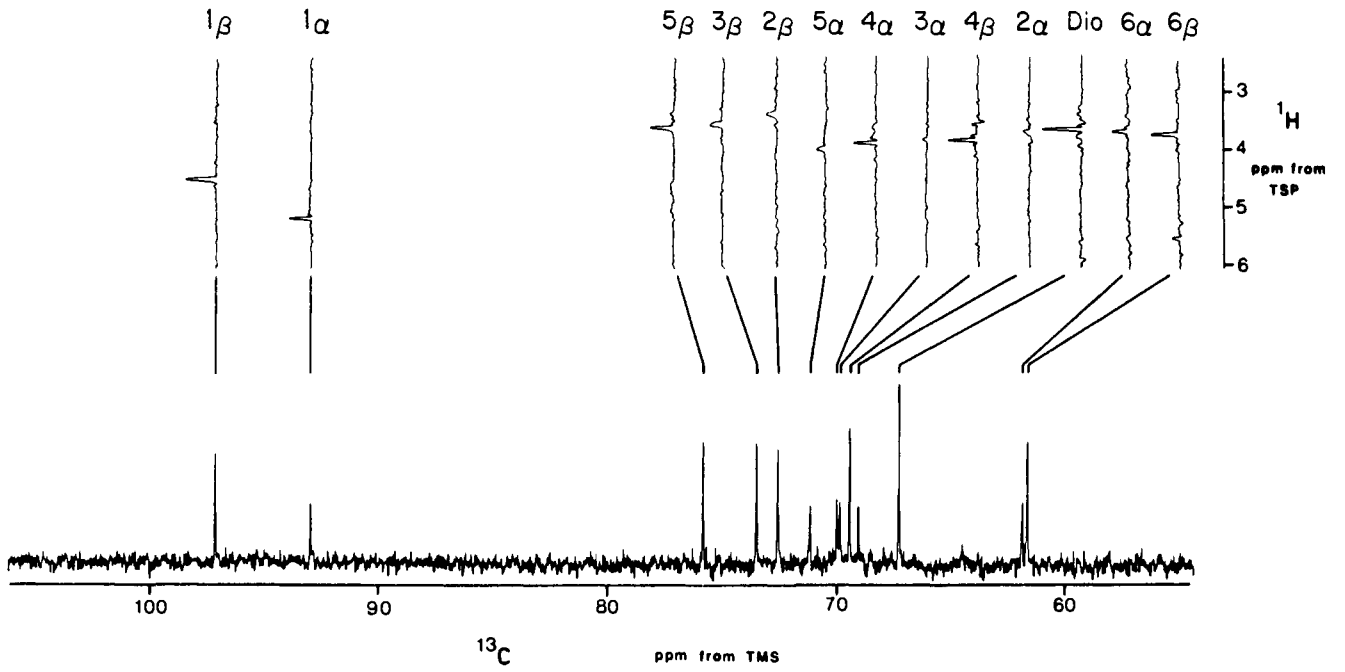

Figure 4. Experimental results for D-galactopyranose (II). The proton-decoupled carbon-13 spectrum is shown horizontally, with traces through the f_1 domain of the 2D spectrum for each protonated carbon resonance displayed vertically.

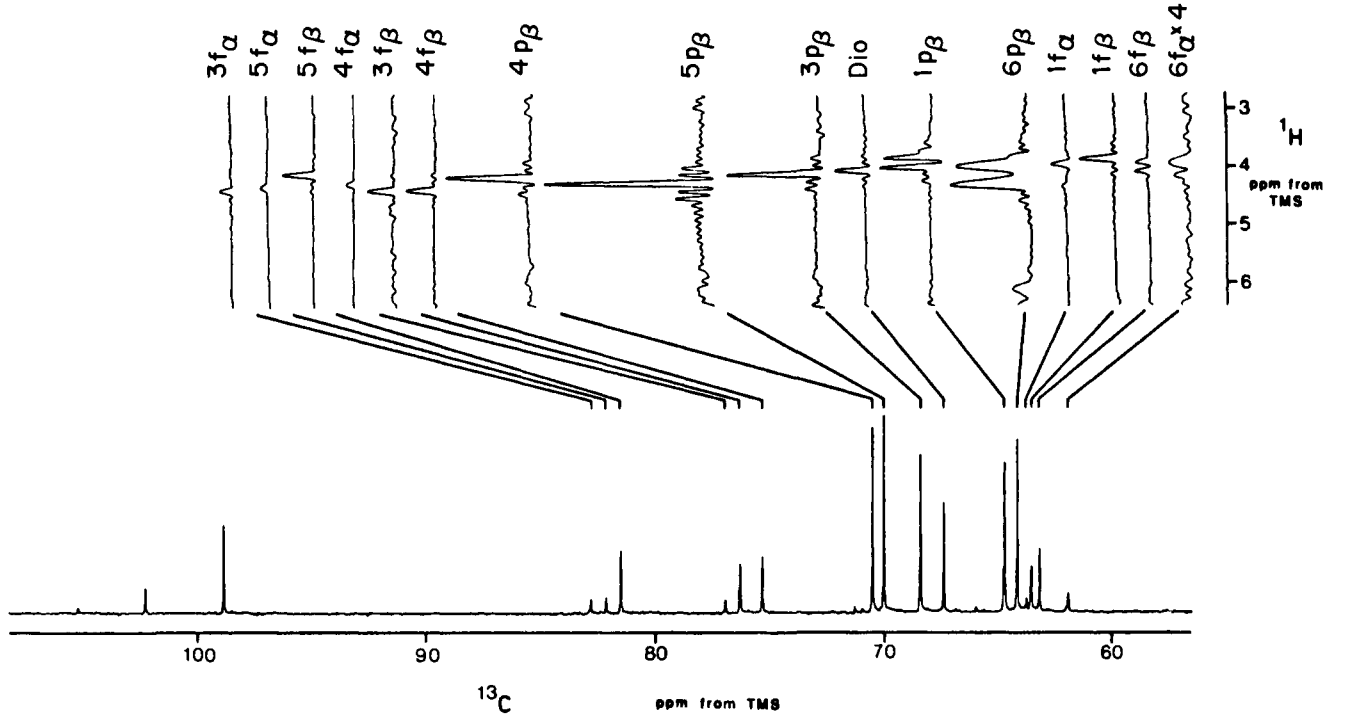

Figure 5. Experimental results for D-fructose (III). Assignments refer to fructose (f) and pyranose (p) forms. The proton-decoupled carbon-13 spectrum is shown horizontally, with traces through the f_1 domain of the 2D spectrum for each protonated carbon resonance displayed vertically.

NTCFT control program of a Nicolet 1180/293A' computer system, equipped with a Diablo model 31 magnetic disk unit. Carbon-13 presaturation was used to reduce artifacts due to imperfect carbon-13 pulses; phase alternation on successive transients would have been more effective, but would have required modification of the otherwise standard control software. The carbon-13 probe system gave a routine signal-to-noise ratio of about 45:1 ASTM (60% deuterobenzene, 1 Hz line broadening) with single phase detection, the carbon-13 and proton radiofrequency field strengths being $\nu_1 = 9$ kHz and $\nu_2 = 4$ kHz, respectively. These specifications leave generous room for improvement. Samples were spun in 10 mm, diam. tubes, all measurements being made at 22 ± 2 °C.

All the sugars were obtained commercially and used without further purification, as 10% anhydrous sugar by weight in D_2O (Merck, Sharp and Dohme), with 2 or 3 drops of dioxane (Fisher) added as chemical shift reference. The suppliers of the sugars were Pfanstiehl (raffinose), Eastham (melibiose), Fisher (sucrose and glucose), Merck (galactose), and BDH (fructose). All of the reducing sugars were allowed to reach equilibrium in solution before use.

Results

The full two-dimensional chemical shift correlation spectrum for raffinose is shown in Figure 3, together with zero-filled traces extracted at each of the protonated carbon-13 chemical shift frequencies, showing the proton signals for each of the carbon sites. Since these traces summarise the information content of the correlation spectrum, full 2D plots are not given for the other systems studied, a plot such as Figure 3 requiring about 1 h of plotting time. Instead the results for three of the six sugars studied are shown in Figures 4 to 6 as conventional decoupled carbon-13 spectra, together with one trace extracted from the 2D spectrum for each protonated carbon site, showing the signals of all the

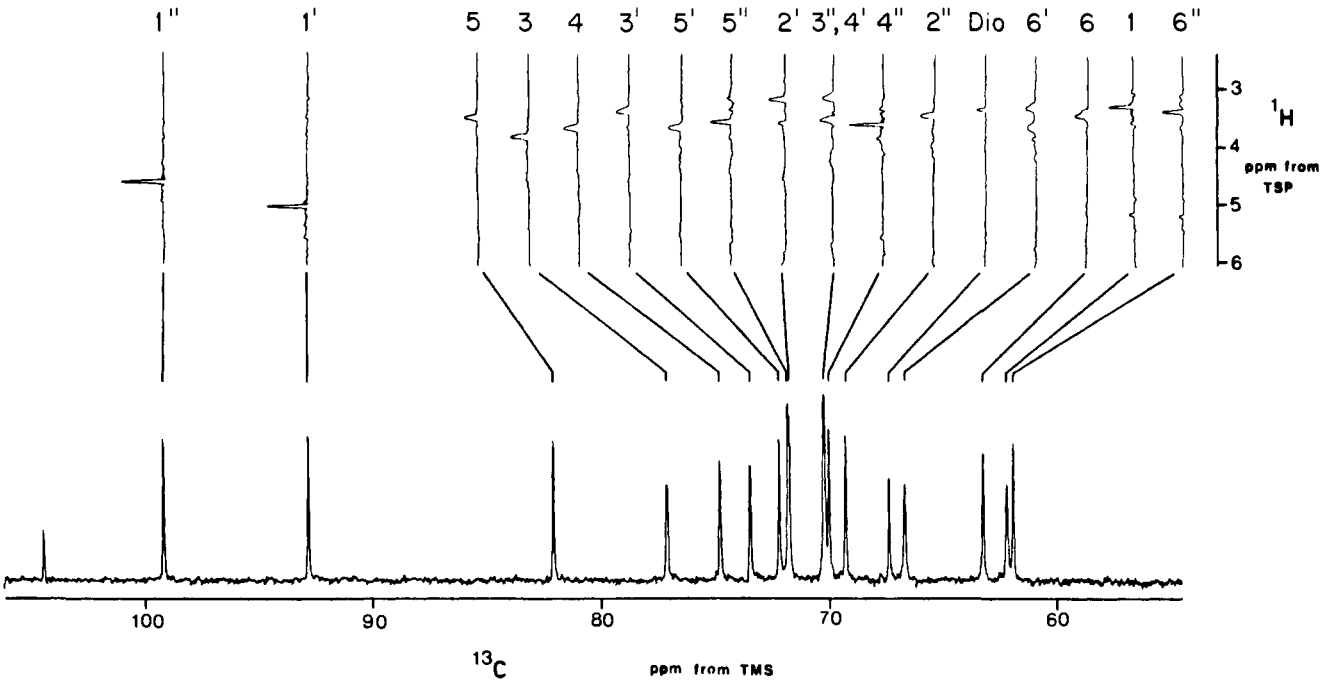

Figure 6. Experimental results for raffinose (VI). The proton-decoupled carbon-13 spectrum is shown horizontally with traces through the f_1 domain of the 2D spectrum for each protonated carbon resonance displayed vertically.

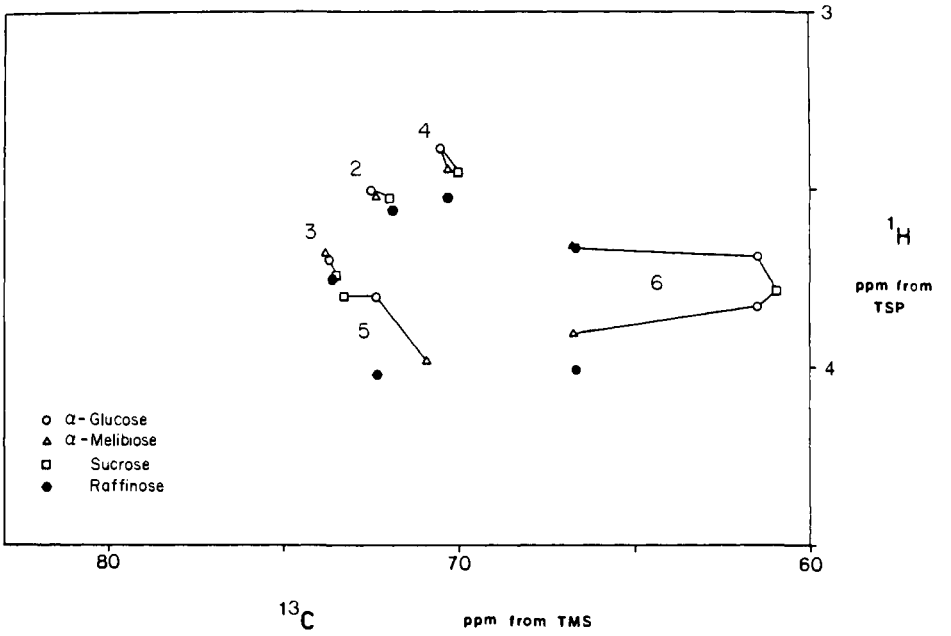

Figure 7. Chemical shift correlation map for the α-D-glucopyranose nonanomeric resonances in free glucose, melibiose, sucrose, and raffinose.

protons directly bound to carbon-13. The chemical shifts measured from the spectra are listed in Table I.

The proton shifts reported in Table I are of intrinsic interest in some cases, due to the difficulty of extracting reliable shift values from the very overcrowded conventional proton spectra of several of these sugars. Most of the proton shifts in these systems have been measured by using continuous wave INDOR at 300 MHz,[7-11] the exceptions being particularly complex or strongly coupled multiplets of the minor anomers and the minor forms of fructose (III). The values given in Table I for α-D-fructofuranose and for most of the resonances of β-D-fructofuranose are believed to be the first reported. The extra resolving power afforded by observing the proton resonances via the carbon signals solves the problem of overcrowding in all the systems studied; the increase in effective resolution greatly exceeds anything to be expected from forseeable improvements in magnet technology. The dynamic range of the shift correlation experiment, although limited by instrument stability and pulse reproducibility, more than suffices for the examination of the weak resonances of α-D-furanofructose[3b] (approximately 10% of fructose is in this form in aqueous solution at room temperature).

The assignments of the carbon-13 spectra of sucrose, galactose, glucose, and fructose have been checked by Pfeffer and coworkers,[3a] using deuterium isotope shifts, thus assigning all the proton shifts in these systems through the experimental correlation results. The proton shifts of melibiose and raffinose are known from continuous wave INDOR studies;[10,11] with their aid the carbon-13 shifts in these systems can be assigned via the shift correlations, completing the carbon and proton assignments for the six sugars. The assignments for melibiose and raffinose differ materially from those in ref 4 and 5.

Since, however, detailed proton shift assignments for molecules more complex than disaccharides are rarely available, it is instructive to consider the problem of assigning the raffinose resonances without the aid of proton data. The combination of proton and carbon-13 chemical shifts characterises a particular site much

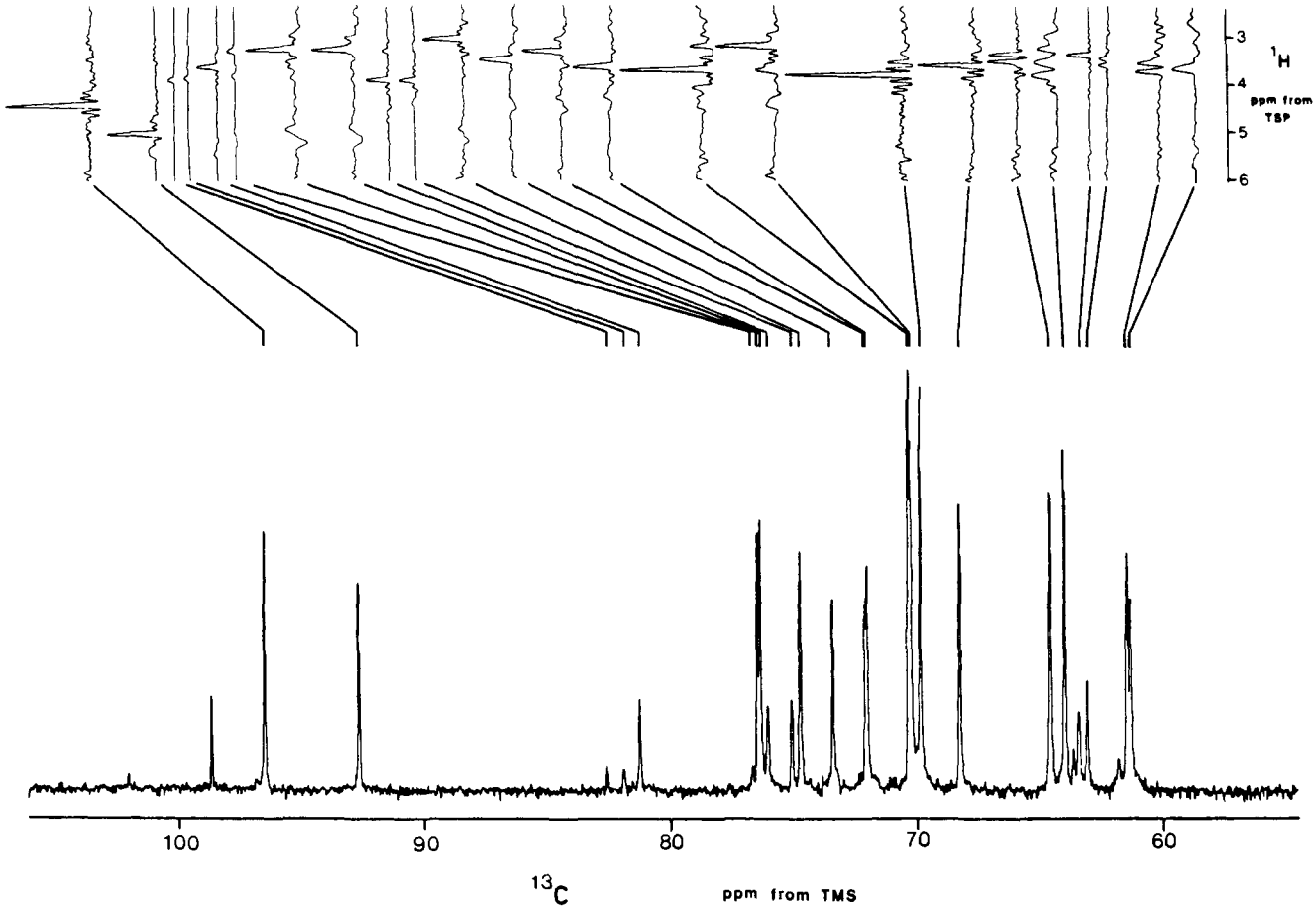

Figure 8. Experimental shift correlation results, in the format of Figures 4–6, for a solution of alfalfa clover honey in D_2O.

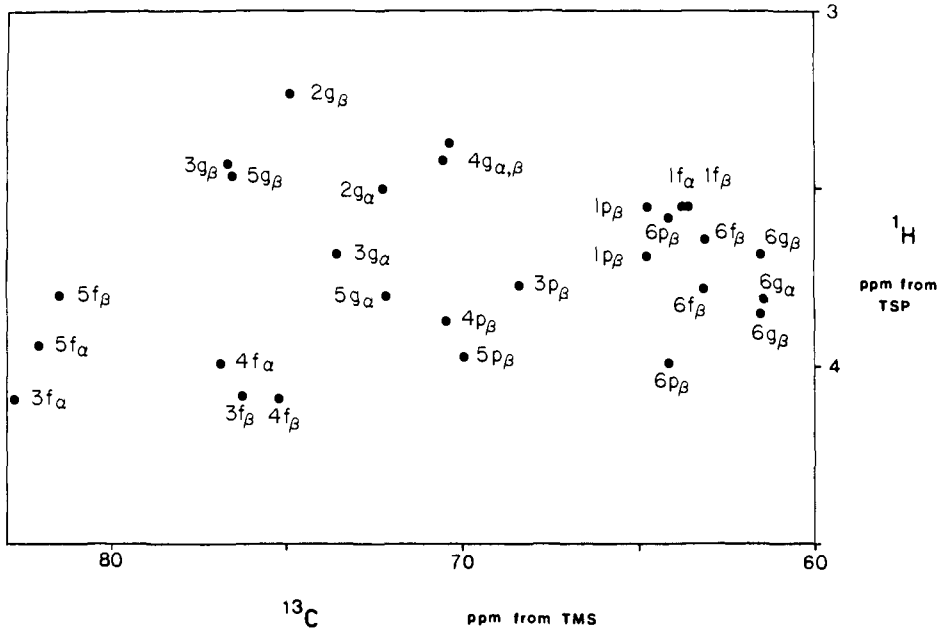

Figure 9. Chemical shift correlation map for the results of Figure 8, showing the assignment of the signals observed to the solution forms of glucose (I) and fructose (III). Glucopyranose signals are denoted by a g, fructopyranose by a p, and fructofuranose by an f; e.g., $2g_\beta$ indicates the C-2 correlation signal of β-D-glucopyranose.

more specifically than a single shift value, allowing a confident assignment of the galactopyranosyl and fructose ring resonances in raffinose on the basis of the analogous shifts in melibiose and sucrose, the effect of adding a third ring being relatively small at the opposite terminus of the trisaccharide. This leaves the central glucopyranosyl ring, in which both the 1→2 linkage to fructose and the 6→1 link to galactose may be expected to cause significant perturbations. For the ring carbons and protons it is reasonable to expect the shift effects to be additive for the addition of the two linkages. That this is indeed the case to an acceptable approximation is most easily appreciated if a map such as Figure 7 is drawn of the carbon-13 and proton shifts of each of the carbon–proton pairs in α-glucose, α-melibiose, sucrose, and raffinose. The displacement of the raffinose glucopyranosyl resonances from those of α-glucose is very close to the vector sum of the glucose–sucrose and glucose–melibiose displacements.

Agreement for the 6-methylene resonances of the galactose–glucose linkage is less good, although still useful, since these shifts show a strong conformational dependence which leads to cooperative shift changes when two rings are added to α-glucose.

The improved resolving power and "fingerprint" character of experimental shift correlation maps can also be of use in the analysis of mixtures. Figure 8 shows the results of a chemical shift correlation experiment on a solution of approximately 20% by volume alfalfa clover honey (Kidd Bros. Produce Ltd., Burnaby, British Columbia) in D_2O. These shift correlations are summarized in Figure 9, together with the assignments made by using the data of Table I. As expected the major constituents of the mixture are identified as α-glucose, β-glucose, β-fructopyranose, α-fructofuranose, and β-fructofuranose.

Discussion

The results described here represent the first tentative attempts at the chemical application of heteronuclear chemical shift correlation by two-dimensional NMR. The accuracy of the proton chemical shifts obtained by this technique is partly determined by the length of time available for data acquisition. In the experiments described the compromise chosen between sensitivity and accuracy was to aim for an estimated standard deviation on proton shifts of ±0.01 ppm, which entails an experiment lasting approximately ten times as long as the acquisition of a normal proton-decoupled carbon-13 spectrum. In a few cases (noted in Table I) the accuracy obtainable was degraded by strong coupling effects or poorly resolved signals. Both accuracy and sensitivity of the 2D experiment compare very favorably with off-resonance decoupling[12-18] and heteronuclear INDOR[33] techniques for measuring correlated proton and carbon-13 shifts.[34]

Heteronuclear chemical shift correlation offers a number of advantages over conventional NMR methods. The extra resolving power made available by detecting proton resonances indirectly via the carbon-13 signals allows the measurement of well-resolved proton signals in systems very much more complex than thoe amenable to study by conventional NMR. The improved resolving power should also aid the analysis of complex mixtures, since the number of signals resolvable in a 2D correlation experiment can be orders of magnitude more than those resolvable in a normal proton or carbon-13 spectrum. In assigning the spectra of unknowns or oligomers the availability of correlated proton shifts is perhaps the single most useful adjunct to a decoupled carbon-13 spectrum. The ability to follow both carbon-13 and proton shifts, which often offer complementary information, can be expremely useful in determining substitution patterns, solution conformations, etc.

The spectra presented here are typical of those obtained from aqueous solutions of carbohydrates; it seems reasonable to expect results of similar quality from many other types of systems. The sensitivity of the heteronuclear chemical shift correlation experiment and the utility of its results make it an attractive proposition for investigating systems whose complexity places them beyond the pale of conventional NMR methods. The principal barrier to its widespread use is the need for complex data processing software and good pulse programming facilities. Both of these problems are now dimishing in magnitude as spectrometer hardware improves, and several manufacturers now offer 2D NMR control programs for their instruments.

Acknowledgment. This work was supported by operating grants (A1905 to L.D.H.) from the National Research Council of Canada and by an Izaak Walton Killam Postdoctoral Fellowship to G. A.M. Components for the spectrometer used were purchased with funds provided by the Chemistry Department and by the President's Emergency Research Equipment Fund, both of the University of British Columbia. The expert assistance of Tom Markus in the construction of the spectrometer was warmly appreciated. We thank Dr. Geoffrey Bodenhausen for a preprint of his work.

(34) Since this manuscript was completed Dr. Alan Jones has informed us of his studies of aqueous sucrose using selective $^{13}C-^{1}H$ decoupling: his results (A. J. Jones, P. Hanish, and A. K. McPhail, to be published) are identical within experimental error with those reported here.

Does the Cyclohexyl Cation Exist in the Dilute Gas State? Direct Evidence from a Radiolytic Study

Marina Attinà, Fulvio Cacace,* and Pierluigi Giacomello

Contribution from the University of Rome, 00100 Rome, Italy. *Received February 24, 1981*

Abstract: The isomeric composition of the gaseous $C_6H_{11}^+$ cations obtained via hydride ion abstraction from c-C_6H_{12} has been investigated by allowing the charged species to react in the gas phase with water and analyzing the neutral products formed. The nature and the yields of the major products, cyclohexanol, cyclohexanone, and 1-methylcyclopentanol, and their dependence on the pressure and the composition of the gaseous system provide direct evidence for the existence of the cyclohexyl cation in the dilute gas state, with a lifetime in excess of 10^{-7} s, and confirm its facile rearrangement to the more stable 1-methylcyclopentyl ion.

The *solvated* cyclohexyl cation has long enjoyed a respectable position as a legitimate ionic intermediate in a variety of reactions occurring in solution, such as deamination, solvolytic processes, acid-induced isomerization, etc.[1] The situation, however, is entirely different for the *free* cyclohexyl cation in media of very low nucleophilicity or in the gas phase. Indeed, all attempts to generate c-$C_6H_{11}^+$ ions in superacid solutions invariably failed, the 1-methylcyclopentyl ion being the only species detectable by NMR spectroscopy even at temperatures as low as −100 °C.[2-4]

Understandably, this failure led to the suggestion that the free cyclohexyl cation is inherently unstable, rearranging instantly,[4] or even *before* its actual formation, i.e., in its "incipient" state,[3] into the 1-methylcyclopentyl ion, and this view was extended to the gas state.[5]

(1) Olah, G. A.; Schleyer, P. v. R., Eds. "Carbonium Ions", Wiley-Interscience: New York, 1970; Vol. 2, Chapters 14 and 15.

(2) Olah, G. A.; Bellinger, J. M.; Capas, C. A.; Lukas, J. *J. Am. Chem. Soc.* **1967**, *89*, 2692–4.

(3) Olah, G. A.; Lukas, J. *J. Am. Chem. Soc.* **1968**, *90*, 933–43.

(4) Arnett, E. M.; Petro, C. *J. Am. Chem. Soc.* **1978**, *100*, 5408–16.

0002-7863/81/1503-4711$01.25/0